

**Oxygen permeation in submicrometric  $\text{Ca}_{0.8}\text{Fe}_{0.2}\text{TiO}_{3-\delta}$  ceramics obtained by  
mechanical activation**

A. Shaula<sup>a</sup>, R.O. Fuentes<sup>a,b</sup>, F.M. Figueiredo<sup>a,c,\*</sup>, V.V. Kharton<sup>a</sup>, F.M.B. Marques<sup>a</sup>, J.R.  
Frade<sup>a</sup>,

<sup>a</sup>Department of Ceramics and Glass Engineering, CICECO, University of Aveiro, 3810-193 Aveiro, Portugal.

<sup>b</sup>CINSO-CITEFA-CONICET, J.B. de la Salle 4379, B1603ALO Villa Martelli, Buenos Aires, Argentina.

<sup>c</sup>Science and Technology Dep., Universidade Aberta, R. da Escola Politécnica 147, 1269-001 Lisbon, Portugal.

\* Corresponding author. Department of Ceramics and Glass Engineering, CICECO, University of Aveiro, 3810-193 Aveiro, Portugal. Fax: +351-234-425300; Tel: +351 234 370 263; e-mail: [framos@cv.ua.pt](mailto:framos@cv.ua.pt)

## **Abstract**

Ceramic samples of  $\text{CaTi}_{0.8}\text{Fe}_{0.2}\text{O}_{3-\delta}$  were obtained from mechanically activated mixtures of  $\text{TiO}_2$ ,  $\text{Fe}_2\text{O}_3$  and  $\text{CaCO}_3$  sintered at  $1150^\circ\text{C}$  for 2 h. The ceramics are dense with submicrometric grains with sizes in the order of 100-200 nm and 400-600 nm. X-ray diffraction analysis revealed a single perovskite phase structure indicating a high level of homogeneity, which was confirmed by transmission electron microscopy. It is found that the oxygen permeability flux of these samples, measured in the range  $700\text{-}950^\circ\text{C}$ , is about 50% lower than for ceramics with considerably larger grains, close to  $10\ \mu\text{m}$ . Moreover, the permeability increases linearly with the increase of the grain size in the range from  $\approx 200\ \text{nm}$  to  $\approx 10\ \mu\text{m}$ . These experimental observations suggest that the grain boundaries have a negative impact on the high temperature ionic transport properties of  $\text{CaTi}_{0.8}\text{Fe}_{0.2}\text{O}_{3-\delta}$  ceramics.

## 1. Introduction

Iron substituted calcium titanate is a candidate for application as a ceramic membrane for oxygen separation due to an attractive combination of properties, including ionic and electronic conductivities, thermal expansion, thermo and chemical stability under large ranges of temperature and oxygen partial pressure and low cost<sup>1-6</sup>. Within the  $\text{CaTi}_{1-x}\text{Fe}_x\text{O}_{3-\delta}$  system, the most attractive is the  $x \approx 0.20$  essentially because of the transport properties<sup>1-8</sup>. The substitution of  $\text{Ti}^{4+}$  by  $\text{Fe}^{3+}$  up to approximately 20 mol.% of iron leads to the formation of oxygen vacancies and thus to significant increase of the ionic conductivity; on the other hand, electrons are injected at low oxygen partial pressure, and electron holes (coupled to the existence of  $\text{Fe}^{4+}$  in oxidising conditions) in both cases leading to increased electronic conductivity<sup>7</sup>. For  $x \geq \approx 0.2$ , the oxygen vacancies tend to order around tetraordinated  $\text{Fe}^{3+}$ <sup>9-11</sup> and a marked decrease in the oxygen conductivity is observed<sup>8,10</sup>, and thus in the oxygen permeability<sup>5,6</sup>.

The material is usually obtained by conventional ceramic route which have a tendency to yield agglomerated powders with compositional inhomogeneities and demands for relatively large sintering temperatures (not less than 1320°C for  $\text{CaTi}_{0.8}\text{Fe}_{0.2}\text{O}_{3-\delta}$ ) in order to obtain an impervious ceramic body<sup>1,2,7,12</sup>. Core-shell grains tend to develop in  $\text{CaTi}_{0.8}\text{Fe}_{0.2}\text{O}_{3-\delta}$ , with grain interiors consisting of pure  $\text{CaTiO}_3$  and the periphery of an iron-substituted phase<sup>12</sup>. This is particularly evident for samples sintered for relatively short periods of time, c.a. 10 h at 1320°C, while still apparent for annealing times as large as 40 h. Although the presence of such inhomogeneities does not seem to decrease performance<sup>12</sup>, it represents an additional uncontrolled factor which may be misleading while trying to assess the effect of the grain size in the ionic conductivity<sup>12</sup>.

On the other hand, the interest for nanosized ceramics has been increasing as they may present properties different from those of normal ceramics with grain sizes in the micron range. The mechanochemical synthesis is certainly an attractive alternative to obtain nano-, or submicrometric, ceramics. Pure  $\text{CaTiO}_3$  has been indeed obtained by grinding  $\text{TiO}_2$  and  $\text{CaO}$  or  $\text{CaCO}_3$  <sup>13</sup>. These powders are nano-crystalline and offer excellent sinterability. Alternatively, the simpler mechanical activation (without direct mechanosynthesis) using milder milling conditions may suffice to bring the precursor initial thermodynamic state to a far from equilibrium state, usually amorphous, which can then be heat treated to obtain the desired phase at a temperature lower than that needed in a conventional ceramic route.

This article reports on the synthesis of  $\text{CaTi}_{0.8}\text{Fe}_{0.2}\text{O}_{3-\delta}$  from mechanically activated  $\text{TiO}_2$ ,  $\text{Fe}_2\text{O}_3$  and  $\text{CaCO}_3$  precursors aiming to obtain dense, homogeneous  $\text{CaTi}_{0.8}\text{Fe}_{0.2}\text{O}_{3-\delta}$  submicrometric ceramics, and on subsequent oxygen permeation studies. Results are presented in comparison to those obtained for ceramics with larger grains obtained via the conventional ceramic route.

## 2. Experimental

The appropriate amounts of high purity powders of anatase  $\text{TiO}_2$ ,  $\text{CaCO}_3$  (Merck) and  $\text{Fe}_2\text{O}_3$  (Riedel-de-Haën) and were mixed in ethanol using a ball mill during 2 h at 20 rpm and dried in air at 60°C. These mixtures were then mechanically activated at room temperature by dry grinding in a Philips PW 4018 planetary ball mill at 500 rpm. The reactants were milled in a 45 cm<sup>3</sup> tetragonal stabilised zirconia (TZP) container and using TZP balls (8 mm in diameter) with a ball to powder weight ratio of 10:1. The grinding was interrupted every 20 min to remove the powder from the wall of the containers. Ceramic

samples were obtained from powders isostatically pressed at 200 MPa and subsequent sintering in air at a maximum temperature of 1150°C for two hours. Two additional temperature dwells of 1 h at 300°C and 700°C were necessary to allow the release of gases resulting from decomposition of the raw materials, mainly CaCO<sub>3</sub>; the heating rate was 2 K/min. The density, measured by immersion in Hg, was higher than 93% of the theoretical density. The microstructure of the ceramic samples was analysed by SEM (Hitachi S4100). The structure and phase purity was monitored *in situ* at various temperatures by powder X-ray diffraction (X'Pert MPD Philips diffractometer with CuK<sub>α</sub> X-radiation). The thermogravimetric and differential thermal analysis (SETARAM TG-DTA LabSys) provided fundamental information for the design of the appropriate sintering curve. A detailed description of the processing procedures will be given elsewhere<sup>14</sup>.

The oxygen permeability was measured using the usual system consisting of an oxygen sensor and an oxygen electrochemical pump, both of stabilised zirconia, sealed onto the membrane under analysis<sup>4-6</sup>. The oxygen gradient across the sample membrane is established between atmospheric air (P<sub>O<sub>2</sub></sub>=21 kPa) at the feed side (P<sub>2</sub>), and a lower value (typically from 15 down to 1.3 kPa) at the permeate side (P<sub>1</sub>), obtained by pumping oxygen out of the chamber. The zirconia sensor is used to monitor P<sub>1</sub> according to the Nernst law. In a steady state condition, the current in the zirconia pump (I<sub>pump</sub>) equals the ionic current entering the chamber through the sample, and thus the molecular oxygen flux, j<sub>O<sub>2</sub></sub> :

$$j_{O_2} = I_{\text{pump}} / (4FS) \quad (1)$$

where  $S$  is the surface area of the membrane available for transport. The measurements were carried out at temperatures in the range 700 to 950°C. The gas tightness of the ceramic samples was verified by forcing a flow of compressed air ( $\approx 250$  kPa) through the membrane under water and checking that no bubbles form on the permeate side. The existence of leaks through the seals was assessed by examining the transient response of the cell, as described in refs.<sup>14,15</sup>.

### 3. Results

Fig. 1 shows a powder XRD pattern of the mechanically activated precursor mixture collected *in situ* at 1000°C. It can be seen that the perovskite phase is formed and no secondary phases are apparent. Note that for non-activated precursors the desired single perovskite material can only be obtained at temperatures higher than 1250°C and over considerably large periods of time ( $> 20$  h)<sup>1,4,10</sup>.

However, the density of the activated ceramics sintered at 1000°C is rather low. Slightly higher temperatures were thus used to avoid oxygen leaks through the membrane during the permeability measurements. The SEM microstructures presented in Fig 2 show that, indeed, the density of ceramics obtained at 1150°C for two hours is rather high and that the few existing pores are not percolated. This result indicates that the activated powders are thus clearly more reactive, and represents a decrease in the densification temperature, when compared to the conventionally prepared samples, of about 200°C<sup>1,4,7,12</sup>. Moreover, it shows that at such low sintering temperature, the ceramics retain a grain size in the submicrometric range. A more detailed analysis has revealed that the size of the majority of the grains falls in the 150-200 nm range, while some larger grains (about 500 nm) are also observed, probably as a result of agglomerates in the initial powders.

It may be concluded that the mechanical activation of the precursor is indeed suitable to obtain ceramics with improved sinterability while retaining the possibility of designing the microstructure by appropriate manipulation of the sintering conditions and/or the activation procedures. Note that the work now shown represents a first attempt and the results obtained therefrom may be further improved.

Fig. 3 shows oxygen permeability data obtained at different temperatures for the 1mm thick membrane, which microstructure is shown in Fig. 2. The flux of molecular oxygen measured between air and 2.1 kPa of oxygen in the permeate side is  $\approx 7.33 \times 10^{-9}$  mol $s^{-1}cm^{-2}$  at 900°C and about one order of magnitude lower at 700°C. These values are considerably lower than those obtained for ceramics with larger grains. For example, the flux is about 30% higher at 900°C for ceramics with an average grain size of 9  $\mu m$ <sup>1-3,12</sup>. Such trends are observed in a relatively broad temperature range, and follow an Arrhenius-like behaviour with apparent activation energy of 117 kJmol<sup>-1</sup> (Fig. 4). This value is closer to that found for the ionic conduction in coarse-grained ( $\approx 10 \mu m$ ) CaTi<sub>0.8</sub>Fe<sub>0.2</sub>O<sub>3- $\delta$</sub> <sup>12</sup> and, thus, the oxygen permeability through the CaTi<sub>0.8</sub>Fe<sub>0.2</sub>O<sub>3- $\delta$</sub>  submicrometric membranes should be mainly determined by the oxygen ion diffusion.

A linear relation is revealed when plotting the flux, for a given oxygen gradient, as a function of the average grain size of the ceramics (Fig. 5). Assuming that the flux is determined essentially by the ionic conductivity and that the conductivity of the grain interior should be independent of the grain size, the results now reported are indicative of resistive nature of the grain boundaries with respect to oxygen transport.

## References

- <sup>1</sup>Iwahara, H., Esaka, T., Mangahara, T., Mixed conduction and oxygen permeation in the substituted oxides for  $\text{CaTiO}_3$ , *J. Appl. Electrochem*, 1988, **18**, 173-177.
- <sup>2</sup>Esaka, T., Fujii, T., Suwa, K., Iwahara, H., Electrical conduction in  $\text{CaTi}_{1-x}\text{Fe}_x\text{O}_{3-\delta}$  under low oxygen pressure and its application for hydrogen production, *Solid State Ionics*, 1990, **40/41**, 544-547.
- <sup>3</sup>Itoh, H., Asano, H., Fukuroi, K., Nagata, M., Iwahara, H., Spin coating of a  $\text{Ca}(\text{Ti,Fe})\text{O}_3$  dense film on a porous substrate for electrochemical permeation of oxygen, *J. Am. Ceram. Soc.*, 1997, **80** [6], 1359-1365.
- <sup>4</sup>Kharton, V.V., Figueiredo, F.M., Kovalevsky, A.V., Viskup, A.P., Naumovich, E.N., Jurado, J.R., Frade, J.R., The Oxygen Diffusion in, and Thermal Expansion of,  $\text{SrTiO}_{3-\delta}$ - and  $\text{CaTiO}_{3-\delta}$ -Based Materials, *Defect and Diffusion Forum*, 2000, **186-187**, 119-136.
- <sup>5</sup>Figueiredo, F.M., Soares, M.R., Kharton, V.V., Naumovich, E.N., Waerenborgh, J.C., Frade, J.R., Properties of  $\text{CaTi}_{1-x}\text{Fe}_x\text{O}_{3-\delta}$  ceramic membranes, *J. of Electroceramics*, in press.
- <sup>6</sup>Figueiredo, F.M., Kharton, V.V., Viskup, A.P., Frade, J.R., Surface Enhanced Oxygen Permeation in  $\text{CaTi}_{1-x}\text{Fe}_x\text{O}_{3-\delta}$  Ceramic Membranes, *J. Membrane Science*, in press.
- <sup>7</sup>Sutija, D., Norby, T., Osborg, P.A., Kofstad, P., AC van der Pauw Measurements of the Electrical Conductivity of Iron-Doped Calcium Titanate; pp. 552-561 in Proc. of the 3<sup>rd</sup> Int. Symposium on Solid Oxide Fuel Cells, *Electrochem. Soc. Proc.*, Vol. 93-4. Eds. S.C. Singhal and H. Iwahara. Electrochemical Society, Pennington, NJ, 1993.
- <sup>8</sup>Figueiredo, F.M., Waerenborgh, J.C., Kharton, V.V., Nafe, H., Frade, J.R., On the relationships between structure, oxygen stoichiometry and ionic conductivity of  $\text{CaTi}_{1-x}\text{Fe}_x\text{O}_{3-\delta}$  ( $x=0.05, 0.20, 0.40, 0.60$ ), *Solid State Ionics*, 2003, **156**, 371-381.



- <sup>9</sup>Grenier, J.-C., Schiffmacher, G., Caro, P., Pouchard, M., Hagenmuller, P., Etude par Diffraction X et Microscopie Electronique du Système CaTiO<sub>3</sub>-Ca<sub>2</sub>Fe<sub>2</sub>O<sub>5</sub> (Study of the CaTiO<sub>3</sub>-Ca<sub>2</sub>Fe<sub>2</sub>O<sub>5</sub> System by X-Ray Diffraction and Electron Microscopy), in French, *J. Solid State Chem.*, 1977, **20**, 365-379.
- <sup>10</sup>McCammon, C., Becerro, A.I., Langenhorst, F., Angel, R., Marion, S., Seifert, F., Short-range Ordering of Oxygen Vacancies in CaFe<sub>x</sub>Ti<sub>1-x</sub>O<sub>3-x/2</sub> Perovskites (0 < x < 0.4), *J. Phys. Condens. Matter*, 2000, **12**, 2969-2984.
- <sup>11</sup>Waerenborgh, J.C., Figueiredo, F.M., Jurado, J.R., Frade, J.R., Fe<sup>4+</sup> Content and short-range ordering of anion vacancies in partially reduced AFe<sub>x</sub>Ti<sub>1-x</sub>O<sub>3-y</sub> (A = Ca, Sr; x ≤ 0.6) perovskites. An <sup>57</sup>Fe Mössbauer spectroscopy study, *J. Phys. Condens. Matter*, 2001, **13**, 8171-8187.
- <sup>12</sup>Figueiredo, F.M., Kharton, V.V., Waerenborgh, J.C., Viskup, A.P., Naumovich, E.N., Frade, J.R., Influence of microstructure on the electrical properties of iron-substituted calcium titanate ceramics, *J. Amer. Ceram. Soc.*, in press.
- <sup>13</sup>Mi, G., Saito, F., Suzuki, S., Waseda, Y., Formation of CaTiO<sub>3</sub> by grinding from mixtures of CaO or Ca(OH)<sub>2</sub> with anatase or rutile at room temperature, *Powder Technology*, 1998, **97-2**, 178-182.
- <sup>14</sup>Fuentes, R.O., Chinarro, E., Figueiredo, F.M., Soares, R., Marques, F.M.B., Frade, J.R., Processing of submicrometric Ca<sub>0.8</sub>Fe<sub>0.2</sub>TiO<sub>3-δ</sub> ceramics by mechanical activation, submitted.
- <sup>15</sup>Figueiredo, F.M., Frade, J.R., Marques, F.M.B., On the accuracy of electrochemical permeability measurements, *Solid State Ionics*, 1998, **110**, 45-53.
- <sup>16</sup>Figueiredo, F.M., Frade, J.R., Marques, F.M.B., Electrochemical permeability of GCO: estimation of overpotentials, *Ionics*, 1999, **5**, 8-12.

## Figures captions

Fig. 1. Powder X ray diffraction pattern collected *in situ* at 1000°C (the \* peaks correspond to the platinum)

Fig. 2. Microstructure of ceramics sintered at 1150°C for 2 hours

Fig. 3. Oxygen electrochemical permeability measured at different temperatures

Fig. 4. Temperature dependence of the oxygen permeability flux measured for ceramics with different grain size (results for the samples with larger  $G_{av}$  were taken from ref.<sup>12</sup>)

Fig. 5. Oxygen permeability flux as function of the average grain size  $G_{av}$  (results for the samples with larger  $G_{av}$  were taken from ref.<sup>12</sup>)

Figures

Fig. 1

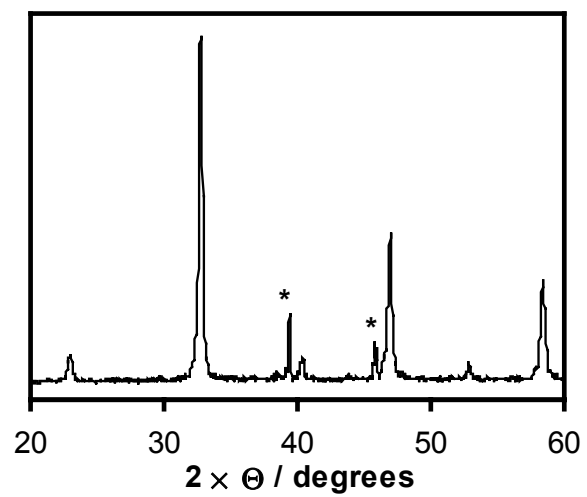


Fig. 2

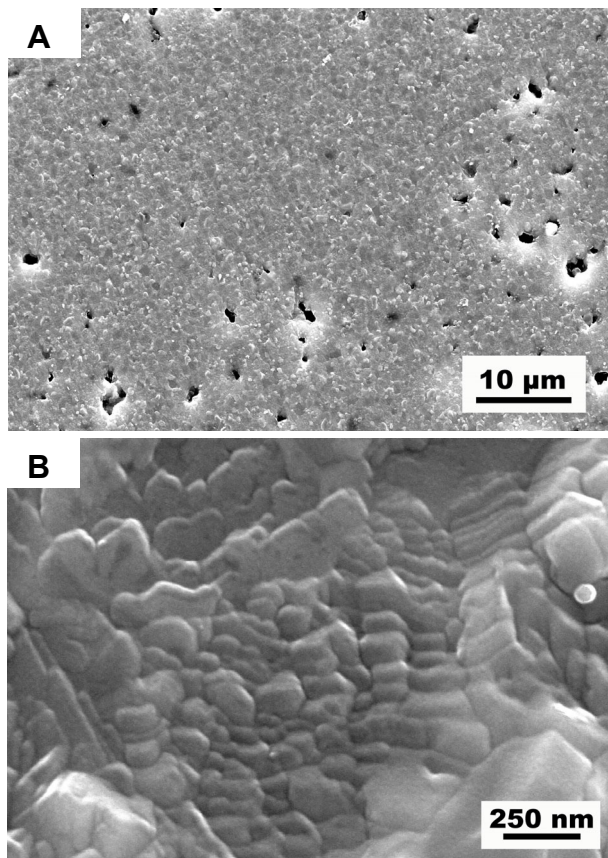


Fig. 3

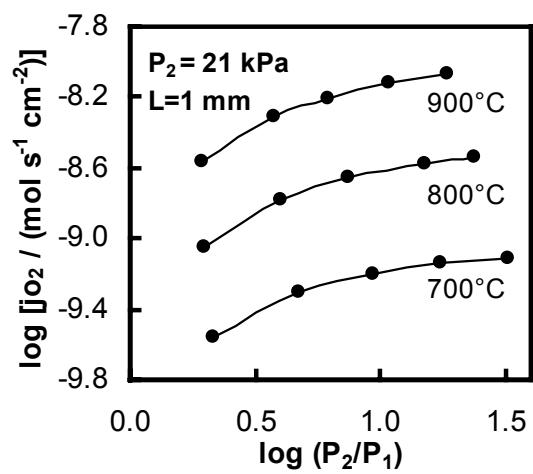


Fig. 4

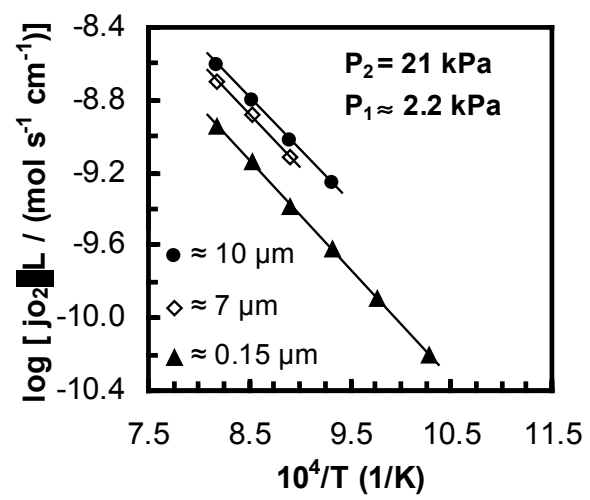


Fig. 5

